

## A generalized anisotropic diffusion for defect detection in low-contrast surfaces

Shin-Min Chao<sup>1,2</sup>, Du-Ming Tsai<sup>1</sup>, Wei-Chen Li<sup>1</sup>, Wei-Yao Chiu<sup>1</sup>

<sup>1</sup>Department of Industrial Engineering and Management, Yuan-Ze University, Taiwan, R.O.C.

<sup>2</sup>Utechzone Co. Ltd., Taiwan, R.O.C  
shinmin@utechzone.com.tw

### Abstract

*In this paper, an anisotropic diffusion model with a generalized diffusion coefficient function is presented for defect detection in low-contrast surface images and, especially, aims at material surfaces found in liquid crystal display (LCD) manufacturing. A defect embedded in a low-contrast surface image is extremely difficult to detect because the intensity difference between unevenly-illuminated background and defective regions are hardly observable. The proposed anisotropic diffusion model provides a generalized diffusion mechanism that can flexibly change the curve of the diffusion coefficient function. It adaptively carries out a smoothing process for faultless areas and performs a sharpening process for defect areas in an image. An entropy criterion is proposed as the performance measure of the diffused image and then a stochastic evolutionary computation algorithm, particle swarm optimization (PSO), is applied to automatically determine the best parameter values of the generalized diffusion coefficient function. Experimental results have shown that the proposed method can effectively and efficiently detect small defects in low-contrast surface images.*

### 1. Introduction

Digital image processing has become a key technology in the area of automated visual inspection (AVI). The manual activity of inspection can be subjective and highly dependent on the experience of human inspectors. Intelligent AVI systems provide significant advantages over traditional human inspection with high process repeatability, accuracy and speed. In this paper, we consider the task of AVI in low-contrast surfaces, and especially focus on the key components used for Thin Film Transistor-Liquid Crystal Displays (TFT-LCDs). The inspection of defects in LCD panel surfaces ensures the display quality and improves the yield in LCD manufacturing.

In a low-contrast surface image, the gray levels of a defect and the background are hardly distinguishable, and there are no clear edges between the defect and its surroundings. For demonstration purposes, Figure 1 presents two low-contrast surface images of backlight panels used for LCD. Figure 1(a) shows a faultless image, and Figure 1(b) shows a defective version of the panel. It can be seen from Figure 1(b) that the defect is difficult to be found in the low-contrast background. In order to visualize the subtle defect, the gray values of the panel images are linearly stretched between 0 and 255 for an 8-bit display. Figures 1(c) and (d) show the contrast-stretched images of Figures 1(a) and (b), respectively. The enhanced defective image shows the defect (marked by a dotted circle) clearly, but it also shows the non-uniformity of the light source and textured pattern of the surface. To solve these problems, one may need complex texture analysis techniques.

There are a few machine vision techniques developed in recent years for defect detection in low-contrast images. Saitoh [1] presented a machine vision scheme for the inspection of brightness unevenness in LCD panel surfaces. An edge detection algorithm was used to identify discontinuous points first. A genetic algorithm was then applied to extract the boundary of anomalous brightness region. Kim et al. [2] studied the detection of spot-type defects in LCD panel surfaces. An adaptive multiple-level thresholding method based on the statistical characteristics of the local area is applied to segment the defect from the background surface. Lee and Yoo [3] proposed a surface fitting approach to identify uneven brightness blemish in

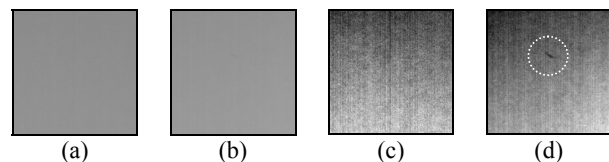


Figure 1. Surface images of backlight panels with low-contrast intensities: (a), (b) faultless and defective images; (c), (d) contrast-stretched images of (a) and (b), respectively.

LCD panels. A bivariate polynomial model was used to estimate the background surface.

In this paper, an anisotropic diffusion scheme is proposed to detect the subtle defects in low-contrast surface image. Anisotropic diffusion model was first introduced by Perona and Malik [4] in image processing for scale-space description and edge detection. The approach is basically a modification of the linear diffusion (or heat equation), and the continuous anisotropic diffusion is given by

$$\frac{\partial I_t(x,y)}{\partial t} = \mathbf{div}[c_t(x,y) \cdot \nabla I_t(x,y)] \quad (1)$$

where  $I_t(x,y)$  is the image at time  $t$ ,  $\mathbf{div}$  the divergence operator,  $\nabla I_t(x,y)$  the gradient of the image and  $c_t(x,y)$  the diffusion coefficient. The diffusion coefficient  $c_t$  is generally selected to be a nonnegative function of gradient magnitude so that small variations in intensity such as noise or shading can be well smoothed, and edges with large intensity transition are distinctly retained. The model can only smooth noise, but cannot intensify low-contrast edges.

In this paper, we propose an anisotropic diffusion model with a generalized diffusion coefficient function to detect defects in low-contrast surface images. The proposed method can distinctly enhance low-contrast defects and uniformly smooth the background without intensifying textured patterns and uneven illumination so that a simple binary thresholding can be effectively applied to segment defects in the diffused image.

## 2. Adaptive anisotropic diffusion model

### 2.1. Perona-Malik anisotropic diffusion

Let  $I_t(x,y)$  be the gray-level at coordinates  $(x,y)$  of a digital image at iteration  $t$ , and  $I_0(x,y)$  the original input image. The continuous anisotropic diffusion in eq. (1) can be discretely implemented by using four nearest neighbors and the Laplacian operator [4]:

$$I_{t+1}(x,y) = I_t(x,y) + \frac{1}{4} \sum_{i=1}^4 [c_t^i(x,y) \cdot \nabla I_t^i(x,y)] \quad (2)$$

where  $\nabla I_t^i(x,y)$ ,  $i = 1, 2, 3$  and  $4$ , represent the gradients of four neighbors in the north, south, east and west directions, respectively.  $c_t^i(x,y)$  is a function of the gradient  $\nabla I_t^i(x,y)$  in the Perona-Malik model, i.e.,

$$c_t^i(x,y) = g(\nabla I_t^i(x,y))$$

For the sake of simplicity,  $\nabla I_t^i(x,y)$  is subsequently denoted by  $\nabla I$ . The function  $g(\nabla I)$  should result in low coefficient values at image edges that have large gradients, and high coefficient values for pixels within an image region with low gradients. In the Perona-Malik anisotropic diffusion model, a possible diffusion coefficient function is given by

$$g(\nabla I) = 1/[1 + (|\nabla I/K|)^2] \quad (3)$$

where the parameter  $K$  is a constant, and must be fine-tuned for a particular application. Parameter  $K$  in the diffusion coefficient function acts as an edge strength threshold. If the  $K$  value is too large, the diffusion process will over-smooth and result in a blurred image. In contrast, if the  $K$  value is too small, the diffusion process will stop the smoothing in early iterations and yield a restored image similar to the original one.

The classical Perona-Malik model only stops the smoothing process in image areas with large gradient magnitude. Therefore, it cannot effectively enhance the subtle defects in a low-contrast image. The parameter value of  $K$  must be manually and empirically determined for different surface patterns.

### 2.2. Generalized diffusion coefficient function

In this paper, we propose a generalized diffusion coefficient function based on a linear-logarithmic function. It controls the function curve by changing the parameter values of the linear-logarithmic function so that different function curves can be flexibly used for different diffusion applications. The proposed generalized diffusion coefficient function  $g(\nabla I)$  is given by

$$g(\nabla I) = \alpha \cdot \ln(|\nabla I| + \beta) + \gamma \quad (4)$$

where  $\alpha$ ,  $\beta$  and  $\gamma$  are curve parameters. Parameter  $\alpha$  is the slope of the linear-logarithmic function, which determines the increment ( $\alpha > 0$ ) or decrement ( $\alpha < 0$ ) of the function. A decreasing diffusion coefficient provides both smoothing and sharpening effects for the image and, therefore, the parameter value of  $\alpha$  is always negative in this study. A larger value of  $|\alpha|$  will result in a larger sharpening effect.

Parameter  $\gamma$  is the intercept of the linear-logarithmic function, which gives the starting diffusion coefficient value of  $g(\nabla I)$  at  $\nabla I = 0$ . A larger value of  $\gamma$  will provide a strong smoothing effect, whereas a smaller value of  $\gamma$  will give a weak smoothing effect. Offset

$\beta$  controls the curvature of the function curve, which can fine-tune the speed of the diffusion process. As  $\beta$  value is increased, the diffusion coefficient value will be slowly decreased.

As a demonstration test image, Figure 1(b) displays the image of a defective backlight panel. Figure 1(d) is the enhanced version of the test image. Figure 2 shows the diffusion results of the test image using three different combinations of the parameters  $\alpha$ ,  $\beta$  and  $\gamma$ . The number of iterations is set to 20 for the test image. With curve parameters  $(\alpha, \beta, \gamma) = (-0.3, 0.1, 0.4)$ , the low-contrast defect cannot be enhanced in the resulting image, as seen in Figure 2(b). With  $(\alpha, \beta, \gamma) = (-0.4, 0.5, 0.2)$ , Figure 2(d) shows that the proposed diffusion model over-sharpens the image. By using  $(\alpha, \beta, \gamma) = (-0.8, 1, 0.9)$ , the diffusion model presents a good diffusion result, as seen in Figure 2(c). The experiment on the test image reveals that the success of the diffusion process for defect detection in low-contrast images critically relies on the proper choice of the parameter values of the generalized diffusion coefficient function.

### 3. Automatic parameters search

To automatically determine the parameter values of  $\alpha$ ,  $\beta$  and  $\gamma$  in the linear-logarithmic function, a performance measure must be given. It should generate an optimal objective value for the best combination of  $\alpha$ ,  $\beta$  and  $\gamma$  that can properly sharpen defects and smooth the background. In this study, an entropy criterion is proposed as the performance measure of a diffused image. Since the gray-level variation is small in the original low-contrast image, the second-order derivative of the gray-level function is used for measuring the complexity in the diffused image. It is desired that both over-smoothed and over-sharpened images result in higher entropy values, and the best diffused image generates a minimum entropy value.

In this study, the objective function that finds the best combination of parameter values of  $\alpha$ ,  $\beta$  and  $\gamma$  for the linear-logarithmic diffusion coefficient function is modeled as

$$\begin{aligned} \text{Minimize } H(I_T) &= -\sum_{\alpha, \beta, \gamma} \sum_x \sum_y L_T(x, y) \cdot \ln L_T(x, y) \\ \text{subject to } &\alpha < 0, \beta > 0 \text{ and } \gamma > 0. \end{aligned} \quad (5)$$

where  $H(I_T)$  is the entropy criterion of an image  $I_T$  at diffusion iteration  $T$ .  $L_T(x, y)$  is the normalized

Laplacian of the diffused image at a given number of diffusion iterations  $T$ , and is given by

$$L_T(x, y) = \frac{|\nabla^2 I_T(x, y)|}{\sum_u \sum_v |\nabla^2 I_T(u, v)|} \quad (6)$$

where  $\nabla^2 I_T(x, y)$  is the discrete Laplacian.

As demonstration sample images, Figures 2(e)-(h) show the normalized Laplacian images of Figures 2(a)-(d), respectively. The normalized Laplacian images of the original gray-level image and the over-smoothed diffusion image present complicated image contents and, therefore, both have high entropy values of 8.97 and 8.53, respectively. The normalized Laplacian image of the over-sharpened image in Figure 2(h) also displays a complicated diffusion result with many false defects and results in a high entropy value of 6.83. The diffused image shown in Figure 2(c) apparently has the best detection result. Its corresponding normalized Laplacian image is less complicated than those of the original gray-level image and the over-smoothed and over-sharpened images, and yields a minimum entropy value of 5.80. In this study, the particle swarm optimization (PSO) search algorithm [5] is applied to automatically determine the best parameter values of the generalized diffusion coefficient function.

### 4. Experimental results

In this section, we present experimental results of two different types of low-contrast surface images including backlight panels (non-textured images) and glass substrates (textured images) to evaluate the performance of the proposed diffusion model. All test images are  $200 \times 200$  pixels wide with 8-bit gray levels. The number of diffusion iterations  $T$  was set at 10 for all test images in the experiments.

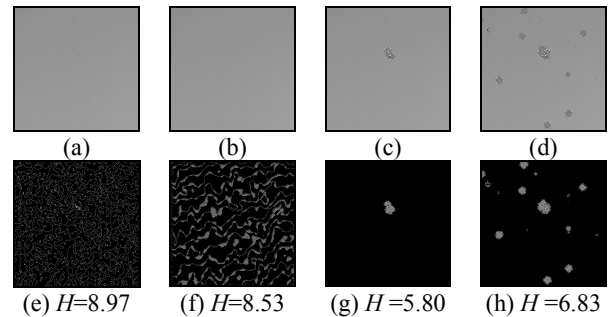


Figure 2. Diffusion results of the defective backlight panel image using different combinations of curve parameters: (a) original defective image; (b)-(d) diffusion results from  $(\alpha, \beta, \gamma) = (-0.3, 0.1, 0.4)$ ,  $(-0.8, 1, 0.9)$  and  $(-0.4, 0.5, 0.2)$ ; (e)-(h) normalized Laplacian images of (a)-(d), respectively.

Figures 3(a)-(c) demonstrate one faultless and two defect images of backlight panel surfaces. Figures 3(d)-(f) present the enhanced images. The results from the proposed diffusion model are presented in Figures 3(g)-(i), which show that all subtle defects are well enhanced in the diffused images. Figures 3(j)-(l) illustrate the thresholding results of the filtered images in Figures 3(g)-(i) as binary images (using the 3-sigma statistical control limits). In the faultless surface image of Figure 3(a), the resulting binary image is uniformly white and no defect is claimed. In the defective images

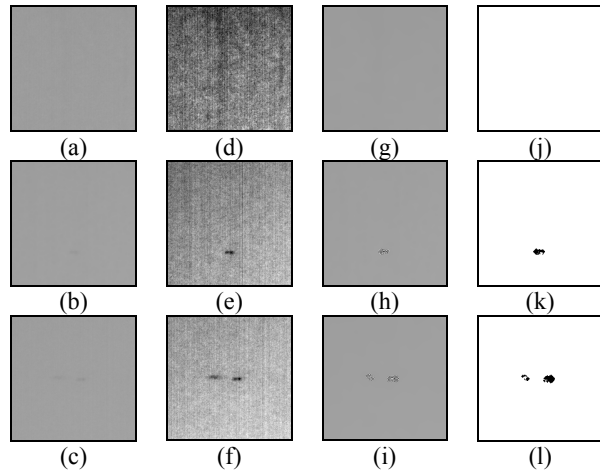


Figure 3. Diffusion results of backlight panel surfaces: (a)-(c) a faultless and two defective test images; (d)-(f) contrast-stretched images of (a)-(c), respectively; (g)-(i) respective diffusion results with  $(\alpha, \beta, \gamma) = (-0.9, 1, 1)$  for all samples; (j)-(l) thresholding results using the 3-sigma control limits.

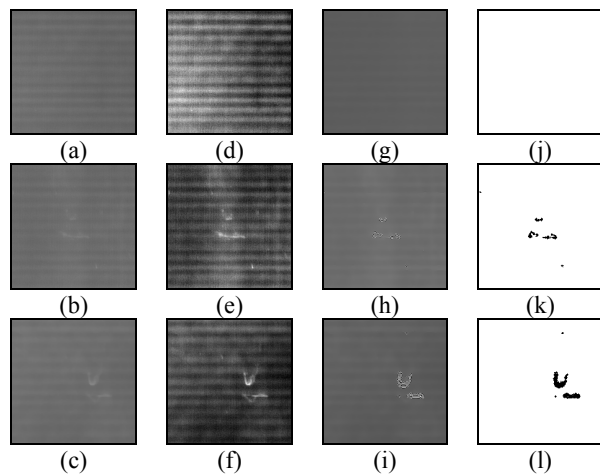


Figure 4. Diffusion results of LCD glass substrates: (a)-(c) a faultless and two defective test images; (d)-(f) contrast-stretched images of (a)-(c), respectively; (g)-(i) respective diffusion results with  $(\alpha, \beta, \gamma) = (-0.6, 1, 0.8)$  for all samples; (j)-(l) thresholding results using the 3-sigma control limits.

of Figures 3(b)-(c), all hardly-visible defects are well detected.

Figure 4 demonstrates further the detection results of LCD glass substrate images that contain horizontal structure patterns on the surfaces. Figure 4(a) is a clear glass substrate image, and Figures 4(b) and (c) are two defective glass substrate images. The enhanced images are shown in Figures 4(d)-(f). The results from the proposed diffusion model are illustrated in Figures 4(g)-(i), which show that the defects are well enhanced and the structural background patterns are smoothed. Figures 4(j)-(l) demonstrate the detection results as binary images using the 3-sigma statistical control limits. The thresholding results also reveal that all local defects embedded in the low-contrast surface images can be effectively detected.

## 5. Conclusion

In this paper, an anisotropic diffusion model with a generalized diffusion coefficient function has been proposed to detect subtle defects in low-contrast, unevenly-illuminated images. The proposed model is flexible to implement for defect detection in various low-contrast surface images by controlling the curve parameter values of the diffusion coefficient function. All parameter values of the model can be automatically determined without human intervention. Experimental results have shown that the proposed diffusion model can be well applied to low-contrast images of backlight panels and LCD glass substrates.

## References

- [1] F. Saitoh, "Boundary extraction of brightness unevenness on LCD display using genetic algorithm based on perceptive grouping factors", *Proceedings of the International Conference on Image Processing*, Kobe, Japan, Oct. 1999, pp. 308-312.
- [2] W.S. Kim, D.M. Kwak, Y.C. Song, D.H. Choi and K.H. Park, "Detection of spot-type defects on liquid crystal display modules", *Key Engineering Materials* 270-273, 2004, pp. 808-813.
- [3] J.Y. Lee, S.I. Yoo, "Automatic detection of region-mura defect in TFT-LCD", *IEICE Trans. Inf. and Syst.*, 2004, pp. 2371-2378.
- [4] P. Perona, J. Malik, "Scale-space and edge detection using anisotropic diffusion", *IEEE Transactions on Pattern Analysis and Machine Intelligence*, 1990, pp. 629-39.
- [5] J. Kennedy, R. Eberhart, "Particle swarm optimization", *Proceedings of the IEEE International Conference on Neural Networks*, Perth, Australia, 1995, pp. 1942-1948.